



Anilido-alldimine aluminum complexes: Synthesis, characterization and lactide polymerization

Laura E.N. Allan^a, Justin A. Bélanger^a, Laura M. Callaghan^a, Donald J.A. Cameron^a, Andreas Decken^b, Michael P. Shaver^{a,*}

^a Department of Chemistry, University of Prince Edward Island, 550 University Avenue, Charlottetown, PE, C1A 4P3, Canada

^b Department of Chemistry, University of New Brunswick, P.O. Box 4400, Fredericton, NB, E3B 5A3, Canada

ARTICLE INFO

Article history:

Received 17 November 2011

Received in revised form

30 January 2012

Accepted 1 February 2012

Keywords:

Aluminum

Lactide

Ligand design

Ring opening polymerization

ABSTRACT

The synthesis of six bimetallic dimethyl aluminum anilido-alldimine complexes, active for the ring opening polymerization of *rac*-lactide, is reported. An efficient synthetic route to these ligands utilizing isolated lithium amide salts allows for the synthesis of novel cyclohexylamide-substituted ligands, as well as improving the yields of diisopropylphenylamino-substituted ligands, with both ethyl and propyl backbones. Less sterically encumbered methylamide-substituted ligands were prepared through the condensation of *ortho*-methylaminobenzaldehyde with the appropriate diamine. A monometallic intermediate species, $L(AlMe_2)$, was isolated and crystallographically characterized, illustrating the preference these ligands display for bis(bidentate) coordination. $L(AlMe_2)_2$ complexes **8–13** are efficient mediators of the ring opening polymerization of *rac*-lactide, with solution polymerizations displaying first-order rate constants, molecular weights very close to the theoretical values and polydispersity indexes as low as 1.07.

© 2012 Elsevier B.V. All rights reserved.

1. Introduction

A recent adaptation of the classic phenoxyimine ligand framework has been the *N*-only donor ligands coined the anilido-alldimines. Replacing the anionic alkoxide donor with an amido functionality has offered different steric and electronic tunability in these systems, however their application and scope remain largely underdeveloped. Ligand frameworks include bidentate [1–3], tridentate [4–7] and bis(bidentate) [8–11] systems, as shown in Fig. 1.

These ligands have been applied to some speciality applications. Dialkylaluminum complexes supported by bidentate ligands exhibit tunable fluorescence in solution and solid state [2], while rare-earth yttrium, scandium and lutetium complexes supported by tridentate ligands were tested as catalysts for the ring-opening polymerization of ϵ -caprolactone and *l*-lactide, exhibiting high activity but only moderate control [4,5]. Magnesium and zinc complexes incorporating tridentate ligands were more effective, polymerizing both ϵ -caprolactone and

l-lactide with polydispersities (PDIs) of 1.1–1.2 [6]. Bis(bidentate) complexes of zinc, mimicking the β -diketiminato complexes developed by Coates et al. [12], have been used successfully to control the copolymerization of epoxides and carbon dioxide [8,9]. Similar bis(bidentate) aluminum and zinc complexes are active catalysts for the living ring opening polymerization of ϵ -caprolactone [11].

Our interest in this ligand set arises from their close relationship to the salen ligand. Aluminum salen complexes were first reported by Spassky et al. and promoted a moderate isotactic bias for the polymerization of lactide ($P_m = 0.68$) [13]. Increased steric bulk improved the isospecificity of the polymerization, with P_m values as high as 0.88 when a 2,4-di(*tert*-butyl)phenol was used [14]. The steric bulk proximal to the active site has been suggested to be the determining factor in promoting chain-end control of polymer tacticity [14,15]. Continued efforts to improve the design of lactide polymerization catalysts is an essential area for growth in polymer science as systems with improved activity or stereocontrol are crucial in developing commercially relevant, sustainable and degradable alternatives to petroleum-derived polymeric materials. In this vein, it was envisaged that moving the bulky *R'* substituents from the *ortho*-substituted aromatic rings of the salen ligand to the amido donor of an anilido-alldimine framework would improve isospecificity (Fig. 2).

* Corresponding author. Tel.: +1 902 566 9375; fax: +1 902 566 0632.

E-mail address: mshaver@upe.ca (M.P. Shaver).

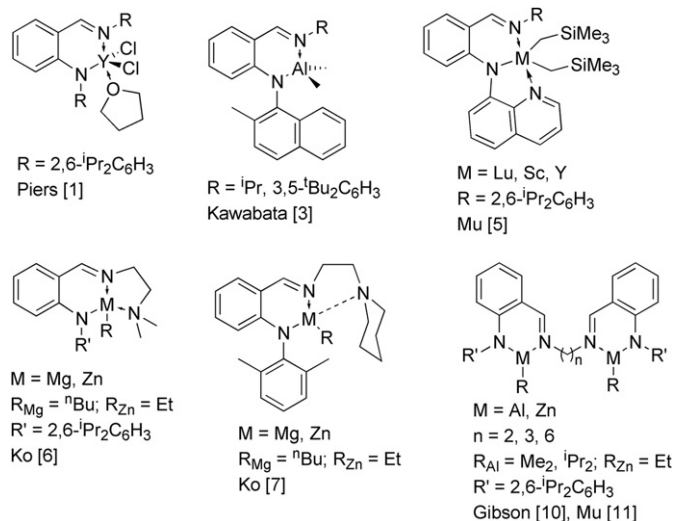


Fig. 1. Anilido-alimine ligands and complexes.

2. Materials and methods

2.1. General experimental procedures

All chemicals and solvents were obtained from Sigma Aldrich in the highest available purity unless otherwise stated. Purasorb *d,l*-lactide and *l*-lactide (PURAC Biomaterials) were sublimed under vacuum three times prior to use. 2,6-diisopropylaniline (90%), benzyl alcohol (99%) and cyclohexylamine were dried over calcium hydride and distilled under a nitrogen atmosphere prior to use. *N,N'*-bis[(2-fluorophenyl)methylene]-1,2-ethanediamine [11], *N,N'*-bis[(2-fluorophenyl)methylene]-1,3-propanediamine [10] and *ortho*-methylaminobenzaldehyde [16] were prepared via previously published procedures. Dry, reagent grade pentane, tetrahydrofuran and toluene were collected from an Innovative Technologies solvent purification system, consisting of columns containing alumina and a copper catalyst. Acetonitrile was dried over calcium hydride and freshly distilled as needed. All solvents were degassed by three consecutive freeze-pump-thaw cycles prior to use. Air-sensitive syntheses were performed in an MBraun Labmaster glovebox equipped with a -35°C freezer and $[\text{O}_2]$ and $[\text{H}_2\text{O}]$ analyzers or under a nitrogen atmosphere on a dual manifold Schlenk line utilizing standard Schlenk techniques. ^1H and ^{13}C NMR spectra were collected on a 300 MHz Bruker Avance Spectrometer. GPC analyses were performed on a PolymerLabs GPC50 system equipped with two Jordi Gel DVB mixed bed columns (300 mm \times 7.8 mm) and a refractive index detector. Samples were dissolved and eluted in HPLC grade THF at a flow rate of 1 mL min $^{-1}$ at 50°C . Molecular weights were measured and corrected relative to styrene standards [17]. Elemental analyses were conducted by Guelph Analytical Laboratories. Crystals of **7** and **9** were grown by precipitation from an acetonitrile solution at -35°C . Single

crystals were coated in Paratone-N oil, mounted using a polyimide MicroMount and frozen in the cold nitrogen stream of the goniometer. A hemisphere of data was collected on a Bruker AXS P4/SMART 1000 diffractometer using ω and θ scans with a scan width of 0.3° and 30 s exposure times. The detector distance was 5 cm. The data were reduced (SAINT) [18] and corrected for absorption (SADABS) [19]. The structure was solved by direct methods and refined by full-matrix least squares on F^2 (SHELXTL) [20] with graphics processed using ORTEP [21]. For **7**, the crystal was a multiple twin and the major component determined. One of the atom positions was disordered and the site occupancies determined using an isotropic model at 0.5 (N(3), N(3')) and fixed in subsequent refinement cycles.

2.2. Synthesis

2.2.1. Ligand synthesis

2.2.1.1. Synthesis of *N,N'*-bis[(2-(2,6-diisopropylphenylamino)benzylidene)]-1,2-ethanediamine (1**).** 3.50 g (19.7 mmol) of 2,6-diisopropylaniline (177.29 g mol^{-1}) was dissolved in 12 mL of tetrahydrofuran. To this stirred solution was added 12.4 mL (19.7 mmol) of *n*-butyllithium (1.6 M solution in hexanes) dropwise. Evolution of heat and gas was observed. Reaction contents were allowed to stir at room temperature for 12 h, at which point an off-white solid was observed. This precipitate was collected by vacuum filtration and utilized without further purification. Yield: 3.25 g (90%). 3.25 g (17.7 mmol) of lithium 2,6-diisopropylanilide (183.22 g mol^{-1}) was added to 40 mL of THF to create a reaction slurry. This mixture was placed in an addition funnel and stored prior to use. Concurrently, 2.19 g (8.1 mmol) of *N,N'*-bis[(2-fluorophenyl)methylene]-1,2-ethanediamine was dissolved in 5 mL of THF in a 125 mL Erlenmeyer flask and cooled to -35°C . The $\text{LiC}_{12}\text{H}_{18}\text{N}$ slurry was then added dropwise to this stirred and chilled solution resulting in the formation of a deep red solution. The reaction was sealed under nitrogen and allowed to stir at room temperature for 12 h. Under an open atmosphere, 20 mL of N_2 -sparged deionized water was added dropwise to the reaction mixture forming an orange suspension. The mixture was poured into a separatory funnel and extracted 3 times with hexanes (100 mL). The organic phase was collected and dried *in vacuo* to yield a yellow oil which was recrystallized from acetonitrile to afford a white product. $\text{C}_{40}\text{H}_{50}\text{N}_4$ (586.40 g mol^{-1}) Yield: 3.56 g (75%). Anal. Calcd for $\text{C}_{40}\text{H}_{50}\text{N}_4$: C, 81.87 H, 8.59; N, 9.55. Found: C, 81.74; H, 8.99; N, 9.35. ^1H NMR (300 MHz, CDCl_3 , 25°C) δ : 10.47 (s, 2H, NH), 8.39 (s, 2H, $\text{HC}=\text{N}$), 7.33–7.20 (m, 4H Ar–H), 7.10 (m, 2H, Ar–H), 7.03 (m, 2H, Ar–H), 6.55 (m, 4H, Ar–H), 6.16 (m, 2H, Ar–H), 3.90 (s, 4H, CH_2CH_2), 3.07 (s, 4H, CH_3CHCH_3), 1.27 (dd, 24H, CH_3 , 5.8 Hz, 3.6 Hz). ^{13}C NMR (75 MHz, CDCl_3 , 25°C) δ : 161.0, 142.3, 138.8, 132.1, 131.3, 127.7, 125.8, 124.4, 123.1, 119.1, 115.7, 62.3, 28.5, 23.5, 23.3.

2.2.1.2. Synthesis of *N,N'*-bis[(2-(2,6-diisopropylphenylamino)benzylidene)]-1,3-propanediamine (2**).** Ligand precursor **2** was prepared analogously to **1** with 3.50 g (19.7 mmol) of 2,6-diisopropylaniline (177.29 g mol^{-1}), 12.4 mL (19.7 mmol) of *n*-butyllithium (1.6 M solution in hexanes) and 2.32 g (8.1 mmol) of *N,N'*-bis[(2-fluorophenyl)methylene]-1,3-propanediamine. $\text{C}_{41}\text{H}_{52}\text{N}_4$ (600.88 g mol^{-1}) Yield: 3.94 g (81%). Anal. Calcd for $\text{C}_{41}\text{H}_{52}\text{N}_4$: C, 81.95 H, 8.72; N, 9.32. Found: C, 81.75; H, 8.90; N, 9.35. ^1H NMR (300 MHz, CDCl_3 , 25°C) δ : 10.42 (s, 2H, NH), 8.42 (s, 2H, $\text{HC}=\text{N}$), 7.33 (m, 2H Ar–H), 7.17 (m, 2H, Ar–H), 7.00 (m, 2H, Ar–H), 6.58 (m, 4H, Ar–H), 6.24 (m, 2H, Ar–H), 3.90 (m, 4H, $\text{CH}_2\text{CH}_2\text{CH}_2$), 3.07 (m, 4H, CH_3CHCH_3), 2.22 (p, 2H, $\text{CH}_2\text{CH}_2\text{CH}_2$, 6.8 Hz, 13.7 Hz), 1.27 (dd, 24H, CH_3 , 5.9 Hz, 3.7 Hz). ^{13}C NMR (75 MHz, CDCl_3 , 25°C) δ : 162.3, 144.7, 138.6, 132.3, 131.3, 128.3, 125.4, 124.6, 123.6, 119.4, 116.1, 62.5, 32.6, 28.9, 23.8, 23.5.

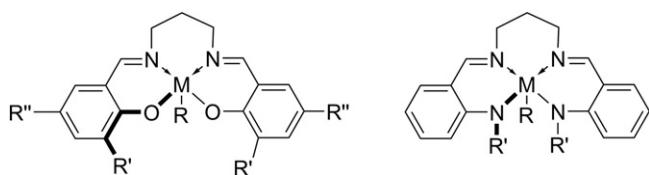


Fig. 2. Proximity of substituent R' to the metal centre in salen and anilido-alimine type ligand frameworks.

2.2.1.3. Synthesis of *N,N'*-bis[(2-(cyclohexylamino)benzylidene)]-1,2-ethanediamine (3**).** Ligand precursor **3** was prepared analogously to **1** with 5.50 g (55.5 mmol) of cyclohexylamine (99.17 g mol⁻¹), 34.7 mL (55.5 mmol) of *n*-butyllithium (1.6 M solution in hexanes) and 3.21 g (11.8 mmol) of *N,N'*-bis[(2-fluorophenyl)methylene]-1,2-ethanediamine. The crude red oil (3.50 g, 80% purity) was loaded on a packed alumina column (25 g) pretreated with 50 mL of 1% (v/v) solution of triethylamine (NEt₃) and hexane. The product was eluted with hexanes (300 mL) to afford an analytically pure yellow oil. C₂₈H₃₈N₄ (430.31 g mol⁻¹) Yield: 2.04 g (40%). Anal. Calcd for C₂₈H₃₈N₄: C, 78.10; H, 8.89; N, 13.01. Found: C, 78.04; H, 9.01; N, 12.95. ¹H NMR (300 MHz, CDCl₃, 25 °C) δ: 9.44 (br s, 2H, NH), 8.37 (s, 2H HC=N), 8.00 (m, 2H, Ar-H), 7.39 (m, 2H, Ar-H), 6.70 (m, 2H, Ar-H), 6.57 (m, 2H, Ar-H), 3.48 (s, 4H, CH₂CH₂), 2.56 (m, 2H, NHCHC₅H₁₀), 2.00–1.05 (m, 20H, 2(C₅H₁₀)). ¹³C NMR (75 MHz, CDCl₃, 25 °C) δ: 162.0, 149.6, 133.8, 133.4, 117.3, 114.6, 113.8, 61.9, 61.2, 33.4, 26.7, 25.1.

2.2.1.4. Synthesis of *N,N'*-bis[(2-(cyclohexylamino)benzylidene)]-1,3-propanediamine (4**).** Ligand precursor **4** was prepared analogously to **1** with 5.50 g (55.5 mmol) of cyclohexylamine (99.17 g mol⁻¹), 34.7 mL (55.5 mmol) of *n*-butyllithium (1.6 M solution in hexanes) and 3.38 g (11.8 mmol) of *N,N'*-bis[(2-fluorophenyl)methylene]-1,3-propanediamine. The crude red oil (3.00 g, 70% purity) was loaded on a packed alumina column (25 g) pretreated with 50 mL of 1% (v/v) solution of triethylamine (NEt₃) and hexane. The product was eluted with hexanes (300 mL) to afford an analytically pure yellow oil. C₂₉H₄₀N₄ (444.33 g mol⁻¹) Yield: 1.57 g (31%). Anal. Calcd for C₂₉H₄₀N₄: C, 78.33; H, 9.07; N, 12.60. Found: C, 78.41; H, 9.10; N, 12.49. ¹H NMR (300 MHz, CDCl₃, 25 °C) δ: 9.41 (s, 2H, NH), 8.34 (s, 2H, HC=N), 7.98 (m, 2H, Ar-H), 7.18 (m, 2H, Ar-H), 6.67 (m, 2H, Ar-H), 6.56 (m, 2H, Ar-H), 3.11 (m, 4H, CH₂CH₂CH₂), 2.55 (m, 2H, NHCHC₅H₁₀), 2.07–1.14 (m, 22H, CH₂CH₂CH₂ and (C₅H₁₀)₂). ¹³C NMR (75 MHz, CDCl₃, 25 °C) δ: 161.7, 149.8, 134.5, 133.2, 117.7, 114.2, 113.6, 62.3, 61.6, 33.1, 33.0, 26.5, 25.4.

2.2.1.5. Synthesis of *N,N'*-bis[(2-(methylamino)benzylidene)]-1,2-ethanediamine (5**).** A solution of *o*-aminobenzaldehyde (3.22 g, 24 mmol) in MeOH (50 mL) was stirred at ambient temperature as 1,2-diaminoethane (0.72 g, 12 mmol) was added dropwise. The yellow solution was heated to reflux for 1.5 h and then stirred at room temperature overnight. The off-white precipitate was collected and recrystallized from MeOH/CHCl₃ to yield a white solid, 2.04 g, 58%. Anal. Calcd for C₁₈H₂₂N₄: C, 73.44; H, 7.53; N, 19.03. Found: C, 73.55; H, 7.64; N, 18.96. ¹H NMR (300 MHz, CDCl₃) δ: 8.91 (br s, 2H, NH), 8.37 (s, 2H HC=N), 7.28 (m, 2H, Ar-H), 7.21 (m, 2H, Ar-H), 6.63 (m, 4H, Ar-H), 3.86 (s, 4H, CH₂CH₂), 2.84 (d, 6H, ²J_{NH} = 5, CH₃) ppm. ¹³C NMR (75 MHz, CDCl₃) δ: 165.4 (HC=N), 150.3, 117.1 (Ar C_q), 133.9, 131.5, 114.2, 109.5 (Ar C-H), 62.4 (CH₂), 29.2 (CH₃) ppm.

2.2.1.6. Synthesis of *N,N'*-bis[(2-(methylamino)benzylidene)]-1,3-propanediamine (6**).** Prepared as for **5** using *o*-aminobenzaldehyde (2.00 g, 15 mmol) and 1,3-diaminopropane (0.55 g, 7 mmol) to yield 1.51 g, 66%. Anal. Calcd for C₁₉H₂₄N₄: C, 73.99; H, 7.84; N, 18.17. Found: C, 74.05; H, 8.00; N, 18.25. ¹H NMR (300 MHz, CDCl₃) δ: 8.97 (br s, 2H, NH), 8.36 (s, 2H HC=N), 7.28 (m, 2H, Ar-H), 7.20 (m, 2H, Ar-H), 6.66 (m, 4H, Ar-H), 3.67 (t, 4H, ³J_{HH} = 7, CH₂CH₂CH₂), 2.94 (d, 6H, ²J_{NH} = 5, CH₃), 2.08 (pentet, 2H, ³J_{HH} = 7, CH₂CH₂CH₂) ppm. ¹³C NMR (75 MHz, CDCl₃) δ: 164.8 (HC=N), 150.4, 117.3 (Ar C_q), 133.9, 131.5, 114.4, 109.7 (Ar C-H), 59.5, 33.1 (CH₂), 29.5 (CH₃) ppm.

2.2.2. Aluminum complex synthesis

2.2.2.1. Synthesis of [1]AlMe₂ (7**).** AlMe₃ (3.0 mL, 1.0 M in toluene, 2.1 mmol) was added dropwise to a solution of **1** (1.76 g, 3.0 mmol)

in 20 mL of toluene at –78 °C. The reaction mixture was held at this temperature for 1 h and then allowed to warm to room temperature and transferred via cannula into an ampoule. The ampoule was sealed under nitrogen and stirred at 80 °C for 12 h, forming a clear yellow solution. Removal of solvent *in vacuo* produced a yellow paste that was recrystallized from acetonitrile to afford **5** in moderate yield. C₄₂H₅₅AlN₄ (642.89 g mol⁻¹) Yield: 1.20 g, 62%. ¹H NMR (300 MHz, CDCl₃, 25 °C) δ: 10.29 (br, 1H, NH), 8.47 (s, 1H, CH=NAr), 8.10 (s, 1H, CH=NAr), 7.30–6.01 (m, 14H, Ar-H), 3.96 (s, 2H, NCH₂), 3.65 (s, 2H, NCH₂), 3.45 (m, 2H, CHCH₃), 3.32 (m, 2H, CHCH₃), 1.54 (d, 12H, CH₃CH), 1.25 (d, 12H, CH₃CH), –0.84 (s, 6H, AlCH₃). ¹³C NMR (75 MHz, CHCl₃, 25 °C) δ: 165.7, 157.0, 142.5, 137.0, 136.1, 133.9, 131.8, 129.1, 128.9, 128.7, 128.5, 126.3, 126.1, 116.0, 115.5, 115.0, 114.7, 69.4, 67.2, 28.7, 28.5, 23.6, 23.3, –8.3.

2.2.2.2. Synthesis of [1](AlMe₂)₂ (8**).** 1.00 g (1.71 mmol) of **1** was dissolved in 3 mL of toluene, in a glass ampoule equipped with magnetic stir bar. To this stirred solution was added 1.71 mL of trimethylaluminum (TMA, 2.0 M solution in heptane), dropwise with stirring. Heat and evolution of gas was observed. The glass ampoule was sealed, removed from glovebox and allowed to stir at 110 °C for 24 h. The volatiles were removed under reduced pressure to reveal an impure orange solid. Washing with pentane gave the aluminum complex in high yield. C₄₄H₆₀Al₂N₄ (698.44 g mol⁻¹) Yield: 0.89 g (75%). Anal. Calcd for C₄₄H₆₀Al₂N₄: C, 75.61; H, 8.65; N, 8.02. Found: C, 75.60; H, 8.47; N, 8.04. ¹H NMR (300 MHz, C₆D₆, 25 °C) δ: 7.67 (s, 2H, HC=N), 7.37–7.06 (m, 8H, Ar-H), 6.82 (d, 2H, Ar-H, 9.0 Hz), 6.34 (t, 2H, Ar-H, 7.0 Hz), 3.90 (s, 4H, CH₂CH₂), 3.48 (m, 4H, CH₃CHCH₃), 1.48 (d, 12H, CH₃, 7.0 Hz), 1.18 (d, 12H, CH₃, 7.0 Hz), –0.33 (s, 12H, Al-CH₃). ¹³C NMR (75 MHz, C₆D₆, 25 °C) δ: 161.0, 142.3, 138.8, 132.1, 131.3, 127.7, 125.8, 124.4, 123.1, 119.1, 115.7, 62.3, 28.5, 23.6, 23.3, –9.1.

2.2.2.3. Synthesis of [2](AlMe₂)₂ (9**).** Prepared as for **8**, using 1.00 g (1.66 mmol) of **2** and 1.66 mL of TMA in 3 mL of toluene. C₄₅H₆₂Al₂N₄ (712.46 g mol⁻¹) Yield: 0.97 g (82%). Anal. Calcd for C₄₅H₆₂Al₂N₄: C, 75.81; H, 8.77; N, 7.86. Found: C, 75.61; H, 8.51; N, 7.75. ¹H NMR (300 MHz, C₆D₆, 25 °C) δ: 7.57 (s, 2H, HC=N), 7.35–7.10 (m, 8H, Ar-H), 6.94 (d, 2H, Ar-H, 9 Hz), 6.43 (t, 2H, Ar-H, 7.0 Hz), 3.90 (m, 4H, CH₂CH₂CH₂), 3.50 (m, 2H, CH₂CH₂CH₂), 3.17 (m, 4H, CH₃CHCH₃), 1.48 (d, 12H, CH₃, 7.0 Hz), 1.18 (d, 12H, CH₃, 7.0 Hz), –0.34 (s, 12H, Al-CH₃). ¹³C NMR (75 MHz, C₆D₆, 25 °C) δ: 162.3, 144.7, 138.6, 132.3, 131.3, 128.3, 125.4, 124.6, 123.6, 119.4, 116.1, 62.5, 32.6, 28.9, 23.8, 23.5, –9.1.

2.2.2.4. Synthesis of [3](AlMe₂)₂ (10**).** Prepared as for **8** using 1.00 g (2.32 mmol) of **3** and 2.32 mL of TMA in 3 mL of toluene. C₃₂H₄₈Al₂N₄ (542.71 g mol⁻¹) Yield: 0.82 g (65%). Anal. Calcd for C₃₂H₄₈Al₂N₄: C, 70.82; H, 8.91; N, 10.32. Found: C, 71.00; H, 8.69; N, 10.50. ¹H NMR (300 MHz, C₆D₆, 25 °C) δ: 7.57 (s, 2H, HC=N), 7.22–7.14 (m, 4H, Ar-H), 6.84 (d, 2H, Ar-H, 8 Hz), 6.42 (t, 2H, Ar-H, 7 Hz), 3.48 (s, 4H, CH₂CH₂), 2.56 (m, 2H, NHCHC₅H₁₀), 2.00–1.05 (m, 20H, (C₅H₁₀)₂), –0.17 (s, 12H, Al-CH₃). ¹³C NMR (75 MHz, C₆D₆, 25 °C) δ: 162.0, 149.6, 133.8, 133.4, 117.3, 114.6, 113.8, 61.9, 61.2, 33.4, 26.7, 25.1, –5.1.

2.2.2.5. Synthesis of [4](AlMe₂)₂ (11**).** Prepared as for **8** using 1.00 g (2.25 mmol) of **4** and 2.25 mL of TMA in 3 mL of toluene. C₃₃H₅₀Al₂N₄ (556.74 g mol⁻¹) Yield: 0.85 g (68%). Anal. Calcd for C₃₃H₅₀Al₂N₄: C, 71.19; H, 9.05; N, 10.06. Found: C, 71.25; H, 9.20; N, 9.96. ¹H NMR (300 MHz, C₆D₆, 25 °C) δ: 7.57 (s, 2H, HC=N), 7.22–7.14 (m, 4H, Ar-H), 6.84 (d, 2H, Ar-H, 8 Hz), 6.42 (t, 2H, Ar-H, 7 Hz), 3.48 (m, 4H, CH₂CH₂CH₂), 3.22 (m, 2H, CH₂CH₂CH₂), 2.56 (m, 2H, NHCHC₅H₁₀), 2.00–1.05 (m, 20H, 2(C₅H₁₀)), –0.17 (s, 12H,

Al–CH₃). ¹³C NMR (75 MHz, C₆D₆, 25 °C) δ : 161.7, 149.8, 134.5, 133.2, 117.7, 114.2, 113.6, 62.3, 61.6, 33.1, 33.0, 26.5, 25.4, –10.4.

2.2.2.6. Synthesis of [5](AlMe₂)₂ (12). 0.50 g (2 mmol) of **5** was dissolved in 15 mL of toluene, in a glass ampoule equipped with magnetic stir bar. 1.18 g of trimethylaluminum (TMA, 2.0 M solution in heptane) was added dropwise, with stirring. Heat and evolution of gas was observed. The glass ampoule was sealed, removed from glovebox and allowed to stir at 110 °C for 24 h. The volatiles were removed under reduced pressure to yield an orange residue which was washed with pentane, filtered and dried under vacuum to give a yellow precipitate. Yield: 0.41 g, 69%. Anal. Calcd for C₂₂H₃₂Al₂N₄: C, 65.01; H, 7.93; N, 13.78. Found: C, 65.30; H, 8.04; N, 13.95. ¹H NMR (300 MHz, CDCl₃) δ : 7.86 (s, 2H, HC=N), 7.33–7.28 (m, 2H, Ar–H), 6.95 (dd, 2H, ³J_{HH} = 8, ⁴J_{HH} = 2, Ar–H), 6.72 (d, 2H, ³J_{HH} = 8, Ar–H), 6.39 (m, 2H, Ar–H), 3.81 (s, 4H, CH₂CH₂), 2.91 (s, 6H, N–CH₃), –0.70 (s, 12H, Al–CH₃) ppm. ¹³C NMR (75 MHz, CDCl₃) δ : 171.7 (HC=N), 157.7, 115.2 (Ar C_q), 137.4, 137.0, 113.4, 113.2 (Ar C–H), 56.7 (CH₂), 33.1 (NCH₃), –9.0 (Al–CH₃) ppm.

2.2.2.7. Synthesis of [6](AlMe₂)₂ (13). Prepared as for **12** using 0.30 g (1 mmol) of **6** and 0.67 g (2 mmol) of TMA in 10 mL of toluene. Yield 0.19 g, 41%. Anal. Calcd for C₂₃H₃₄Al₂N₄: C, 65.69; H, 8.15; N, 13.32. Found: C, 65.73; H, 8.24; N, 13.46. ¹H NMR (300 MHz, CDCl₃) δ : 7.96 (s, 2H, HC=N), 7.37–7.31 (m, 2H, Ar–H), 7.08 (dd, 2H, ³J_{HH} = 8, ⁴J_{HH} = 2, Ar–H), 6.72 (d, 2H, ³J_{HH} = 9, Ar–H), 6.47 (m, 2H, Ar–H), 3.60 (t, 4H, ³J_{HH} = 8, CH₂CH₂CH₂), 2.88 (s, 6H, N–CH₃), 2.20 (pentet, 2H, ³J_{HH} = 8, CH₂CH₂CH₂), –0.75 (s, 12H, Al–CH₃) ppm. ¹³C NMR (75 MHz, CDCl₃) δ : 170.4 (HC=N), 157.6, 120.5 (Ar C_q), 137.2, 136.8, 115.3, 113.2 (Ar C–H), 55.2, 31.1 (CH₂), 33.1 (NCH₃), –9.2 (Al–CH₃) ppm.

2.3. Lactide polymerization

0.020 g of the desired precatalyst (**8–13**), 2.00 M equivalents of benzyl alcohol and 200 M equivalents of *rac*-lactide were added to an oven-dried ampoule charged with a magnetic stir bar and 3 mL of toluene when appropriate. The ampoule was sealed and heated to 120 °C (bulk polymerization) or 70 °C (solution polymerization) with stirring for the desired period of time. The ampoule was cooled to room temperature and the resulting viscous mixture was dissolved in a 10:1 v:v dichloromethane:methanol solution. Once fully dissolved, the solution was left to stir at ambient temperature for 30 min and then precipitated by dropwise addition of the solution into 100 mL of cold methanol. The resulting white precipitate was filtered and dried *in vacuo* to constant weight. Samples were analyzed by ¹H{¹H} NMR spectroscopy and gel-permeation chromatography.

3. Results and discussion

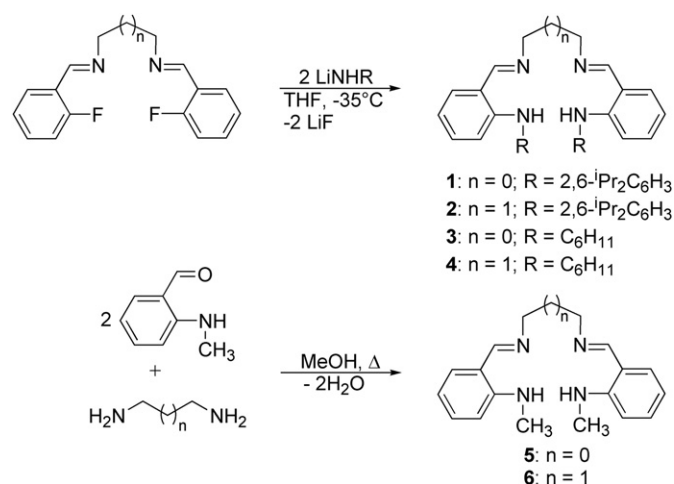
Six potentially tetradentate anilido-alimine ligands were targeted in this study, containing 2,6-diisopropylphenyl, cyclohexyl or methyl substituents on the amine donors and ethyl or propyl chains bridging the imine functionalities. Proligands **1–4** were synthesized by modifying previously reported procedures [10,11], with the fluorinated precursors first prepared via the acid-catalyzed condensation of 2-fluorobenzaldehyde and the appropriate diamine. Controlled addition of lithium 2,6-diisopropylphenylamide or lithium cyclohexylamide to the fluorinated precursor at –35 °C promoted a metathesis reaction, forming the desired products in good yield. Of note, isolation of the lithium amido intermediates was important to maximize ligand yields. This route was unsuccessful for the synthesis of N-methyl substituted ligands, as the reaction of the fluorinated

precursors with lithium methylamide yielded a complex mixture of products which could not be separated. Proligands **5** and **6** were successfully prepared through modification of a literature procedure [16], through the condensation of *ortho*-methylaminobenzaldehyde with the appropriate diamine. The general reaction scheme for ligand synthesis is outlined in Scheme 1.

Purification of **1–4** was challenging, as the solubility of both the ligand and fluorinated precursor precluded a rapid filtration and washing methodology. Slow recrystallization of **1** and **2** from acetonitrile afforded these desired ligands in good yields, while cyclohexyl derivatives **3** and **4** were purified on alumina columns pretreated with a 1% v/v solution of triethylamine (NEt₃) in hexanes to limit ligand binding to the alumina. Ligands **5** and **6** were more straightforward to purify and were recrystallized from a methanol/chloroform mixture. ¹H and ¹³C NMR spectroscopy confirmed product formation and purity, particularly noted by the presence of the NH peak at δ 10.4 ppm (**1**, **2**), δ 9.4 ppm (**3**, **4**) and δ 8.9 ppm (**5**, **6**). In the case of **1–4**, an upfield shift of the imine signals from δ 8.6 ppm in the fluorinated precursors to \sim δ 8.4 ppm in the anilido-alimine proligands was also observed, whereas the appearance of the imine resonances at δ 8.4 ppm confirmed the formation of **5** and **6**.

Aluminum complexes supported by these ligands were prepared via protonolysis of the proligand and trimethylaluminum (TMA). Initial experiments focused on a 1:1 ratio of **1**:TMA. This reaction gave a mixture of products at high (110 °C) and ambient temperatures. Careful interpretation of the ¹H NMR spectrum of crude reaction products suggested that the major product was a bimetallic complex, (L)(AlMe₂)₂. Other products included free ligand and an unknown aluminum-containing species. Lowering the reaction temperature to –78 °C allowed for isolation of the monometallic compound after recrystallization from acetonitrile. NMR and X-ray crystallographic characterization showed that [**1**] AlMe₂, **7**, had formed: the ligand prefers a bidentate coordination mode, with a free pendant arm. A similar structure was prepared purposefully as an intermediate in the preparation of hetero-bimetallic complexes [22]. The molecular structure for **7** is shown in Fig. 3 while relevant bond lengths, angles and crystallographic parameters are given in Tables 1 and 2. Repeated attempts to grow crystals which would yield a higher quality molecular structure were unsuccessful.

As expected, the Al(1)–N(2) bond is shorter than the Al(1)–N(1) bond, confirming the stronger amido-aluminum bond. The imine bond length is short, although significantly elongated by \sim 0.15 Å



Scheme 1. Synthesis of substituted anilido-alimine ligands **1–6**.

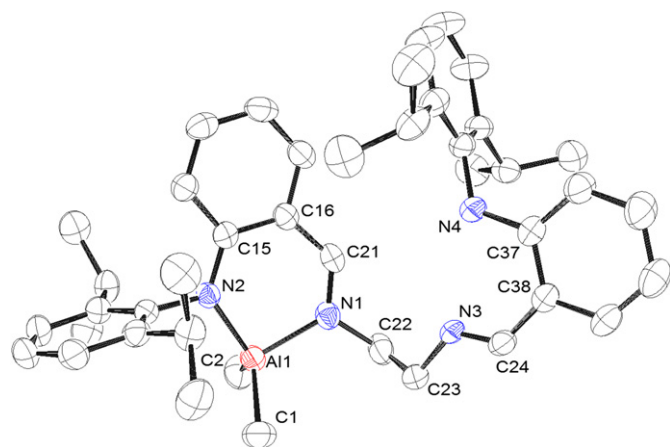


Fig. 3. ORTEP drawing (spheroids at 50% probability) of $[1]\text{AlMe}_2$, **7**. Hydrogen atoms omitted for clarity.

when compared to the unbound imine fragment. Bond angles reveal that chelation of the ligand to the aluminum centre causes a pinching of the ligand framework and a narrowing of the bond angles. This results in a distorted tetrahedral geometry around the aluminum, exemplified by the small $\text{N}(2)\text{--Al}(1)\text{--N}(1)$ bite angle of $94.38(8)^\circ$. ^1H NMR spectroscopy confirms both the monometallic nature of the complex and the pendant arm in solution. Further attempts with **1** and **2–6** to isolate a tetradentate aluminum complex $[\text{L}]\text{AlMe}$ by controlling reaction temperatures, times and concentrations were unsuccessful.

Exclusive formation of the bimetallic complexes $[\text{L}](\text{AlMe}_2)_2$ (**8–13**) is readily achieved by altering the reagent ratio to 1:2 ligand:TMA, greatly improving reaction yields. The complexes are shown in Fig. 4. Complex **8** has been previously reported and crystallographically characterized [11]. For complex **9**, crystals were grown from a saturated acetonitrile solution and analyzed by single crystal X-ray crystallography. The molecular structure for **9** is shown in Fig. 5 while relevant bond lengths, angles and crystallographic parameters are given in Tables 3 and 4. The symmetry observed in the crystal structure ensures the two aluminum centres, and thus catalytically active sites, are equivalent. The bidentate coordination of the anilido-aldimine ligand is maintained, linked by the flexible aliphatic chain to give the bimetallic product. The bond lengths and angles around the metal centres in **9** are nearly unchanged from the monometallic structure **7** and are also similar to related and previously published complexes [10,11].

Table 1
Selected bond lengths and angles for **7** ($[\text{1}]\text{AlMe}_2$).

Atoms	Length (Å)	Atoms	Angle ($^\circ$)
$\text{Al}(1)\text{--N}(1)$	1.9292(18)	$\text{N}(1)\text{--Al}(1)\text{--C}(1)$	110.23(8)
$\text{Al}(1)\text{--N}(2)$	1.8881(18)	$\text{N}(1)\text{--Al}(1)\text{--C}(2)$	104.12(10)
$\text{Al}(1)\text{--C}(1)$	1.958(3)	$\text{N}(2)\text{--Al}(1)\text{--C}(1)$	115.16(10)
$\text{Al}(1)\text{--C}(2)$	1.967(3)	$\text{N}(2)\text{--Al}(1)\text{--C}(2)$	117.58(10)
$\text{N}(1)\text{--C}(21)$	1.295(3)	$\text{N}(2)\text{--Al}(1)\text{--N}(1)$	94.38(8)
$\text{N}(1)\text{--C}(22)$	1.468(3)	$\text{C}(1)\text{--Al}(1)\text{--C}(2)$	112.82(13)
$\text{N}(2)\text{--C}(3)$	1.449(2)	$\text{C}(3)\text{--N}(2)\text{--Al}(1)$	115.25(12)
$\text{N}(2)\text{--C}(15)$	1.369(3)	$\text{C}(15)\text{--N}(2)\text{--Al}(1)$	127.07(13)
$\text{N}(3)\text{--C}(23)$	1.52(4)	$\text{C}(15)\text{--N}(2)\text{--C}(3)$	117.65(16)
$\text{N}(3)\text{--C}(24)$	1.15(3)	$\text{C}(21)\text{--N}(1)\text{--Al}(1)$	123.84(15)
$\text{N}(4)\text{--C}(25)$	1.430(3)	$\text{C}(21)\text{--N}(1)\text{--C}(22)$	118.50(18)
$\text{N}(4)\text{--C}(37)$	1.378(3)	$\text{C}(22)\text{--N}(1)\text{--Al}(1)$	117.25(14)
$\text{C}(16)\text{--C}(21)$	1.429(3)	$\text{C}(24)\text{--N}(3)\text{--C}(23)$	123.0(3)
$\text{C}(22)\text{--C}(23)$	1.506(4)	$\text{C}(24)\text{--N}(3)\text{--C}(23)$	113.0(2)
		$\text{C}(37)\text{--N}(4)\text{--C}(25)$	122.54(17)

Table 2
Crystallographic data and details for **7** ($[\text{1}]\text{AlMe}_2$).

Empirical Formula	$\text{C}_{42}\text{H}_{55}\text{AlN}_4$	Formula weight	642.88
Crystal system	Monoclinic	Space group	$\text{P}2_1/\text{c}$
a, b, c (Å)	13.496(2), 13.913(3), 20.820(5)		
α, β, γ ($^\circ$)	90, 99.431(2), 90		
$V, \text{\AA}^3$	3856.7(13)	Total reflections	25 597
Z	4	Unique reflections	8584
$D_{\text{calc}}, \text{mg m}^{-3}$	1.107	Parameters	437
Wavelength, Å	0.71073	R_1^a	0.1010
T, K	173(1)	wR_2^b	0.1701
θ range ($^\circ$)	1.53–27.50	Goodness-of-fit	1.052

^a $R_1 = \Sigma (F_o - F_c) / \Sigma F_o$.

^b $wR_2 = [\Sigma w(F_o^2 - F_c^2)^2 / \Sigma (wF_o^4)]^{1/2}$.

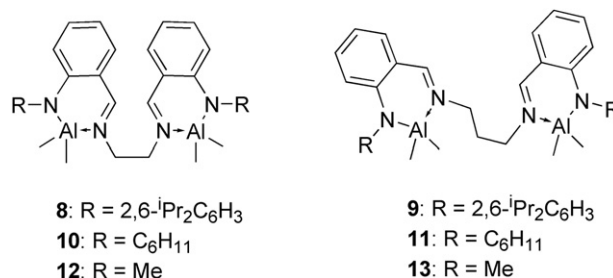


Fig. 4. Bimetallic aluminum complexes **8–13**.

Synthesis of the cyclohexylamido substituted complexes **10** and **11** suggest an even higher propensity to favour the bimetallic complex, despite their reduced steric demands. Reactions of **3** and **4** with one equivalent of TMA showed mixtures of products, including the bimetallic complexes, even at low temperatures. Similar results were obtained when using the least sterically encumbered ligands **5** and **6**, with bimetallic complexes **12** and **13** the major product under all attempted reaction conditions. Synthesis of **10–13** was improved through the use of 2:1 TMA:ligand ratios and high temperatures, affording the desired bimetallic complexes in moderate yields. Diagnostic resonances, such as the AlCH_3 signal at $\delta -0.17$ ppm, and accurate integration supported this assignment. Reaction progress was monitored over time by observing the loss of the NH resonance at $\delta 9.4$ ppm in the ^1H NMR spectra. While the desired monometallic complexes could not be isolated, six bimetallic aluminum alkyl complexes were prepared and tested for the controlled ring-opening polymerization of *rac*-lactide. Interestingly, bimetallic catalysts have been shown to offer improved activity and control over lactide polymerization [23], although reduced stereocontrol would be expected from the more open active site.

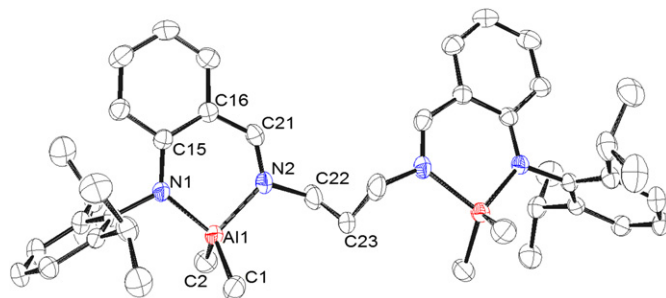


Fig. 5. ORTEP drawing (spheroids at 50% probability) of $[\text{2}](\text{AlMe}_2)_2$, **9**. Hydrogen atoms omitted for clarity.

Table 3
Bond lengths and angles for **9** ($[2](\text{AlMe}_2)_2$).

Bond	Length (Å)	Bond	Length (Å)
N(1)–Al(1)	1.8918(14)	N(1)–Al(1)–N(2)	95.15(2)
N(2)–Al(1)	1.9482(15)	N(1)–Al(1)–C(1)	114.35(8)
Al(1)–C(1)	1.963(2)	N(1)–Al(1)–C(2)	115.45(8)
Al(1)–C(2)	1.965(2)	N(2)–Al(1)–C(1)	112.55(9)
N(2)–C(21)	1.293(2)	N(2)–Al(1)–C(2)	104.90(8)
N(1)–C(15)	1.365(2)	C(1)–Al(1)–C(2)	112.70(11)
N(1)–C(3)	1.445(2)	C(15)–N(1)–Al(1)	127.65(11)
N(2)–C(22)	1.481(2)	C(3)–N(1)–Al(1)	113.89(11)
C(22)–C(23)	1.512(3)	C(21)–N(2)–Al(1)	123.78(12)
C(16)–C(21)	1.436(2)	C(22)–N(2)–Al(1)	117.76(13)

Table 4
Crystallographic data for **9**, $[2](\text{AlMe}_2)_2$.

Empirical Formula	C ₄₅ H ₆₂ Al ₂ N ₄	Formula weight	712.95
Crystal system	Orthorhombic	Space group	Pbcn
a, b, c (Å)	15.7648(16), 17.2749(17), 15.2425(15)		
α , β , γ (°)	90, 90, 90		
V, Å ³	4151.1(7)	Total reflections	27 336
Z	4	Unique reflections	4742
D _{calc} , mg m ^{−3}	1.141	Parameters	355
Wavelength, Å	0.71073	R ₁ ^a	0.0676
T, K	173(1)	R _w ^b	0.1339
θ range (°)	1.75 to 27.50	Goodness-of-fit	1.123

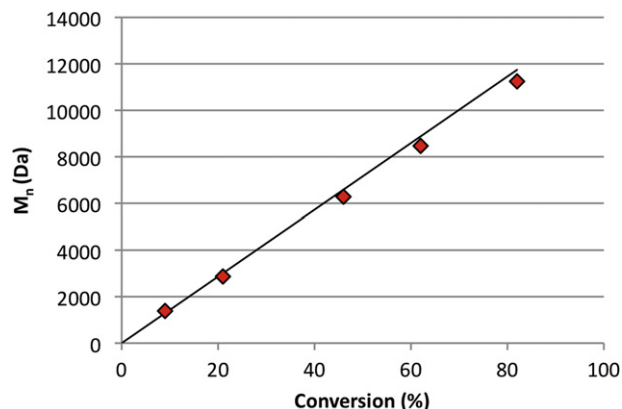
^a $R_1 = \sum (F_o - F_c) / \sum F_o$.^b $wR_2 = (\sum w(F_o^2 - F_c^2)^2 / \sum (wF_o^4))^{1/2}$.

Polymerizations were initiated by the addition of benzyl alcohol, forming the aluminum alkoxide *in situ*, and were carried out in toluene at 70 °C and in molten lactide at 120 °C. Lactide:initiator:catalyst ratios of 200:2:1 were used under the presumption that one active, growing chain per metal centre was the steric limit for these systems. Results are summarized in Table 5. Polymerizations with **7** were uncontrolled and exhibited extremely broad, multimodal PDIs, which can be attributed to the presence of an alternate initiating site on the pendant ligand arm.

Neat polymerizations of lactide mediated by **8–13** are rapid but lack control. High polydispersities and molecular weights are indicative of poor catalyst stability and activity at these high temperatures. However, the same catalysts offer good control over the ROP of *rac*-lactide in toluene at 70 °C, reaching moderate to high conversions in 16 h. Attempts to extend these reactions to higher conversions led to eventual catalyst degradation and transesterification of the polymer. No induction period was noted,

Table 5
Polymerization data for bimetallic anilido-alimine aluminum catalysts (**8–13**) with *rac*-lactide.^a

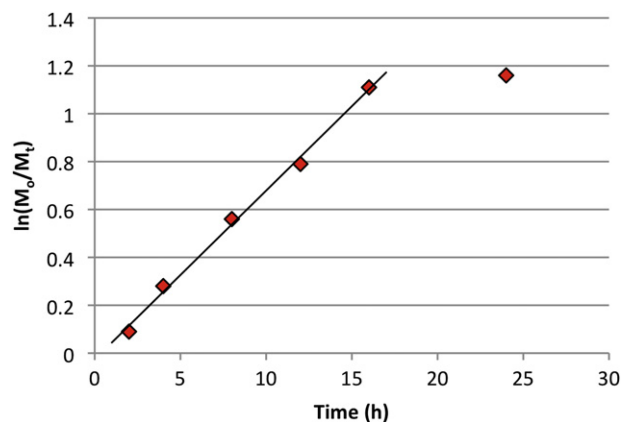
Catalyst	Temp (°C)	Time (hr)	Conv. (%)	$M_{n, \text{GPC}}$	$M_{n, \text{th}}$	PDI
8	70	16	67	9010	9594	1.17
9	70	16	60	9123	8592	1.25
10	70	16	82	11 244	11 742	1.23
11	70	16	65	9034	9308	1.37
12	70	16	66	7324	9322	1.07
13	70	16	58	6780	8701	1.07
8	120	3	82	18 626	9447	1.59
9	120	3	85	30 539	9792	1.64
10	120	3	86	16 132	9908	1.47
11	120	3	78	26 507	8986	1.49
12	120	3	81	11 834	11 416	1.58
13	120	3	91	10 175	13 590	1.56

^a Lactide:benzyl alcohol:catalyst ratio of 200:2:1 employed. GPC molecular weights measured and corrected relative to styrene standards [17].**Fig. 6.** Plot of M_n versus conversion for the solution polymerization of *rac*-lactide at 70 °C by $[3](\text{AlMe}_2)_2$, **10**. Solid line represents theoretical molecular weights.

suggesting the initial protonolysis reaction between the aluminum alkyl species and benzyl alcohol to form the desired alkoxide initiator is rapid relative to propagation in each case. Cyclohexyl-substituted ethyl-bridged catalyst **10** achieved the highest conversions under these conditions. All catalysts displayed living characteristics for these polymerizations, as evidenced by linear plots of M_n vs. conversion with R^2 values higher than 0.98 and low polydispersities. A typical plot is shown in Fig. 6.

The rates of polymerization for these reactions, k_{obs} , were also determined. Plotting $\ln(M_0/M_t)$ versus time for each kinetic run further supported the living nature of these catalysts, but also revealed that little productive polymerization occurs after 16 h of reaction time. Rates ranged from $1.64 \times 10^{-5} \text{ s}^{-1}$ for **9** to $2.80 \times 10^{-5} \text{ s}^{-1}$ for **10**. Interestingly, the rates for the ethyl-bridged catalysts were significantly higher than their propyl-bridged counterparts, a trend opposite to that observed in monometallic aluminum salen systems [14]. A representative plot is given in Fig. 7. The rates of these catalysts are significantly lower than for the fastest aluminum salen initiators which possess first-order rate constants in the range of 10^1 s^{-1} , a six-order of magnitude decrease in our system [24].

In all cases these bimetallic aluminum catalysts (**8–13**) were found to possess no capacity for tacticity control in the polymerization of *rac*-lactide. The selectively decoupled ^1H NMR spectra of the resultant PLA revealed the presence of the five possible tetrads arising from *rac*-lactide, characteristic of an atactic chain. The steric

**Fig. 7.** Plot of $\ln(M_0/M_t)$ versus time for the solution polymerization of *rac*-lactide at 70 °C by $[3](\text{AlMe}_2)_2$, **10**.

influence of the diisopropylphenyl, cyclohexyl and methyl substituents proximal to the metal centre, coupled with the change in ligand electronics, hinders the formation of monometallic aluminum complexes. This promotes the formation of bimetallic aluminum complexes that, while active for polymerization, do not possess the sterically inhibited active site required to promote tacticity control. The open coordination sphere around the metal centre also means that the growing polymer chain is not affected by changes to the ligand framework, resulting in very similar ROP data for complexes **8–13**.

4. Conclusions

An improved synthetic procedure for the synthesis of anilido-alimine ligands has been reported. Use of the isolated lithium amide salts in the metathesis reaction significantly improves the yield of 2,6-diisopropylphenylamino-substituted ligands, from the previously reported 40% to *ca* 80%. This new route has been used to successfully synthesize two novel ligands, with cyclohexylamino substituents. Less sterically encumbered ligands **5** and **6**, with methylamino substituents, were prepared in good yields utilizing the literature method previously reported for **5**. The synthesis of monometallic methyl aluminum complexes was unsuccessful; however, the bimetallic dimethyl aluminum complexes **8–13** were prepared in excellent yields, with complex **9** characterized through X-ray crystallography. Complexes **8–13** are active catalysts for the ROP of *rac*-lactide, with the initiators prepared *in situ* through the addition of benzyl alcohol. Bulk polymerizations at 120 °C are rapid but show poor control, with molecular weights which are much higher than theoretical values and broad PDIs. Solution polymerizations at 70 °C reveal excellent control over both molecular weights and PDIs, with the living nature of the polymerizations illustrated through linear M_n vs conversion plots. Rates are first-order in monomer, with rate constants of $1.64\text{--}2.80 \times 10^{-5} \text{ s}^{-1}$. Current efforts to target monometallic aluminum complexes of anilido-aldimines by varying the ligand's steric influence continue.

Appendix. Supplementary Data

Supplementary data related to this article can be found online at doi:10.1016/j.jorgchem.2012.02.003.

References

- [1] P.G. Hayes, G.C. Welch, D.J.H. Emslie, C.L. Noack, W.E. Piers, M. Parvez, *Organometallics* 22 (2003) 1577–1579.
- [2] X. Liu, W. Gao, Y. Mu, G. Li, L. Ye, H. Xia, Y. Ren, S. Feng, *Organometallics* 24 (2005) 1614–1619.
- [3] K. Hayashi, Y. Nakajima, F. Ozawa, T. Kawabata, *Chem. Lett.* 39 (2010) 643–645.
- [4] X. Shang, X. Liu, D. Cui, J. Polym. Sci. Part A: Polym. Chem. 45 (2007) 5662–5672.
- [5] W. Gao, D. Cui, X. Liu, Y. Zhang, Y. Mu, *Organometallics* 27 (2008) 5889–5893.
- [6] Y.-H. Tsai, C.-H. Lin, C.-C. Lin, B.-T. Ko, J. Polym. Sci. Part A: Polym. Chem. 47 (2009) 4927–4936.
- [7] Y.-C. Liu, C.-H. Lin, B.-T. Ko, R.-M. Ho, J. Polym. Sci. Part A: Polym. Chem. 48 (2010) 5339–5347.
- [8] B.Y. Lee, H.Y. Kwon, S.Y. Lee, S.J. Na, S.-i. Han, H. Yun, H. Lee, Y.-W. Park, *J. Am. Chem. Soc.* 127 (2005) 3031–3037.
- [9] T. Bok, H. Yun, B.Y. Lee, *Inorg. Chem.* 45 (2006) 4228–4237.
- [10] D.J. Doyle, V.C. Gibson, A.J.P. White, *Dalton Trans.* (2007) 358–363.
- [11] W. Yao, Y. Mu, A. Gao, W. Gao, L. Ye, *Dalton Trans.* (2008) 3199–3206.
- [12] M. Cheng, E.B. Lobkovsky, G.W. Coates, *J. Am. Chem. Soc.* 120 (1998) 11018–11019.
- [13] M. Wisniewski, A.L. Borgne, N. Spassky, *Macromol. Chem. Phys.* 198 (1997) 1227–1238.
- [14] P. Hornmair, E.L. Marshall, V.C. Gibson, R.I. Pugh, A.J.P. White, *Proc. Natl. Acad. Sci. USA* 103 (2006) 15343–15348.
- [15] E.L. Marshall, V.C. Gibson, H.S. Rzepa, *J. Am. Chem. Soc.* 127 (2005) 6048–6051.
- [16] M. Green, P.A. Tasker, *J. Chem. Soc. A* (1970) 2531–2539.
- [17] A. Kowalski, A. Duda, S. Penczek, *Macromolecules* 31 (1998) 2114–2122.
- [18] Saint 7.23A, Bruker AXS, Inc, Madison, Wisconsin, USA, 2006.
- [19] SADABS 2008 George Sheldrick, Bruker AXS, Inc, Madison, Wisconsin, USA, 2008.
- [20] G.M. Sheldrick, *Acta Crystallogr. Sect. A: Found. Crystallogr.* A64 (2008) 112–122.
- [21] L.J. Farrugia, *J. Appl. Cryst.* 30 (1997) 565.
- [22] A.-H. Gao, W. Yao, Y. Mu, W. Gao, M.-T. Sun, Q. Su, *Polyhedron* 28 (2009) 2605–2610.
- [23] B.J. O'Keefe, L.E. Breyfogle, M.A. Hillmyer, W.B. Tolman, *J. Am. Chem. Soc.* 124 (2002) 4384–4393.
- [24] A. Bhaw-Luximon, D. Jhurry, N. Spassky, *Polym. Bull.* 44 (2000) 31–38.